



# Investigation of the Ductile Cutting Behavior of Monocrystalline Yttria-Stabilized Zirconia During Ultra-Precision Orthogonal Cutting

Hae-Sung Yoon<sup>1</sup> · Suk Bum Kwon<sup>2</sup> · Aditya Nagaraj<sup>2</sup> · Sangkee Min<sup>2</sup>

Received: 7 December 2018 / Revised: 13 February 2019 / Accepted: 6 May 2019 / Published online: 29 May 2019  
© Korean Society for Precision Engineering 2019

## Abstract

Manufacturability of advanced ceramics has been a challenging issue mainly because of their brittle behaviors and high hardness. One approach to solving this issue is enabling ductile regime cutting, which can also be used to enhance the quality of the surface and accuracy of the final product. There have been many studies investigating how to control and prolong the ductile response regime during cutting; however, it still lacks a straightforward explanation that enables us to predict the transition of the material response from the ductile regime to the brittle regime. In this study, the processing of monocrystalline yttria-stabilized zirconia was investigated to predict material behavior during cutting. Here, it is aimed to confirm that stress intensity factor analysis can be applied with a wide variety of process parameters and investigate the effect of varying the process parameters on the ductile–brittle material response transition. Experimental results showed that negative rake angle and higher cutting speed prolonged the ductile cutting regime. However, the cutting stress at the ductile–brittle transition point remained constant regardless of the process parameters which enabled us to predict the transition point with respect to the stress intensity factor. It is expected that the results of this research can contribute to the development of machining strategies with improved throughput and thus to increasing the utilization of ceramic materials.

**Keywords** Yttria-stabilized zirconia · Brittleness · Stress intensity factor · Ultra-precision machining

## 1 Introduction

Engineering ceramics, such as zirconia (zirconium dioxide, ZrO<sub>2</sub>), sapphire ( $\alpha$ -Al<sub>2</sub>O<sub>3</sub>), and silicon carbide (SiC), are attracting increasing attention from researchers in various industrial fields. Advanced ceramics usually possess great hardness, strength, as well as chemical and thermal stability [1]. Many researchers have investigated the multifunctional performance endowed by their physical/chemical properties, and they are used in a wide variety of applications, such as in the aerospace, automotive, electrical and optics industries. However, it is difficult to fabricate these materials because

conventional processing technologies are not fully applicable due to their low process efficiency [2].

In this paper, the processing of yttria-stabilized zirconia (YSZ) was investigated. Zirconia and zirconia containing ceramics exhibit a high level of fracture toughness/hardness, and low thermal conductivity. Thus, they have been used in various industrial applications including extrusion dies and thermal coating materials. Monocrystalline cubic zirconia is used as a gemstone and diamond simulant because of its crystallographic isometry and high refractive index [3]. Zirconia is known to have three different phases with respect to temperature: monoclinic (<950 °C), tetragonal (1200–2370 °C), and cubic (> 2370 °C) [4]. These can cause large volumetric changes during fabrication processes. Other oxide materials, such as yttrium oxide (Y<sub>2</sub>O<sub>3</sub>), magnesium oxide (MgO), and calcium oxide (CaO), are commonly added to prevent this crystal polymorphism and stabilize the crystal structures. These dopants can stabilize zirconia in either its tetragonal or cubic crystal form, depending on the composition of the material and the processing temperature [5].

✉ Sangkee Min  
sangkee.min@wisc.edu

<sup>1</sup> School of Aerospace and Mechanical Engineering,  
Korea Aerospace University, 76 Hangeongdaehak-ro,  
Deogyang-gu, Goyang-Si, Gyeonggi-do 10540, South Korea

<sup>2</sup> Department of Mechanical Engineering, University  
of Wisconsin-Madison, 1513 University Avenue, Madison,  
WI 53706, USA

However, like other engineering ceramics, it is difficult to fabricate zirconia because of its brittleness and hardness. In particular, it is easy to cause undesired cracks on the surface, subsurface damage, and excessive tool wear when machining these materials [2]. Ductile regime cutting has been investigated and used as an approach to resolve these issues. Depending on the scale of the deformation, temperature, pressure conditions, etc., ductile behavior can be obtained as the dominant response of the material to cutting [6, 7]. This behavior can significantly enhance the surface clarity without causing the machined surface to crack. Thus, maintaining and prolonging the ductile regime during cutting may offer a plausible solution to better quality surfaces and more accurate products.

Many studies have been performed to investigate and explain the ductile behavior of ceramics in various machining processes, from single-point scratching to grinding [8]. Researchers have observed the machining characteristics of various ceramic materials [9], analyzed the sizes of surface cracks and subsurface damage [10], and even used assisted machining techniques to further their understanding of ductile regime cutting [11]. From the perspective of modeling, Venkatachalam et al. [12], presented a comprehensive model to predict ductile cutting behavior in terms of the stress intensity factor and fracture toughness. The authors assumed varying shear plane angle and simulated cutting forces with respect to various process parameters. Then they performed a comparison of simulation and experiments mainly in terms of undeformed chip thickness. On the other hand, Arif et al. [13] formulated a model and explained the transition of the material response in terms of the fracture energy. Authors in the above literature considered lateral and median cracks during the cutting and assumed brittle fracture energy in terms of crack lengths.

Though many modelling studies have been performed, it is still not straightforward to predict and control ductile regime cutting, because the response of the material during the cutting has not yet been fully understood and explained, mainly with respect to crystallographic information. The machining characteristics of single crystal materials vary with the cutting direction because their response is influenced significantly by the structure and orientation of the crystals. Anisotropic mechanical properties complicate the analysis further. In particular, the multiple deformations and fracture behaviors during cutting cause issues in the case of conventional machining processes, such as milling.

In light of this, studies have been performed to investigate and analyze in detail the behavior during orthogonal cutting of single crystal materials. Mizumoto et al. [14] analyzed

the anisotropic machining behavior of monocrystalline sapphire in terms of its crystallographic planes and inherent deformation mechanisms. They calculated the ductile/brittle deformation parameters based on geometric projections of the critical resolved shear stress and fracture energy for different cutting directions. Based on this study, Yoon et al. [15] investigated the machining characteristics of single crystal sapphire in various cutting directions along the four primary crystal planes. The authors analyzed the stress intensity factor at the point where the response of the material transitioned from the ductile regime to the brittle regime (herein referred to as the ductile–brittle transition point) with respect to the cutting directions on different planes. The same approach was also used to observe the machining characteristics in orthogonal cutting of 8 mol% YSZ in a cubic crystal form Yoon et al. [16]. Distinctive crack morphologies corresponding to different crack-opening planes were observed. The measured cutting forces at the ductile–brittle transition point agreed well with the values estimated based on the critical stress intensity factor projected in each cutting direction. These studies basically aimed to find crack initiation parameters based on given material properties and crystal orientations, so that a model could be formulated to predict the dominant material response. The studies mentioned above showed that projecting the stress intensity factor in the direction normal to the corresponding crystal plane (or on a mode I fracture direction) matched the critical stress intensity factor of each plane well.

However, further research is required to fully predict the response of the material to cutting with a wide variety of parameters. The studies described above mainly focused on anisotropic machining behavior in terms of crystal orientation only. Though they showed good agreement between their experimental and analytical results, they only explained the anisotropic tendencies of ductile cutting behavior under specific cutting conditions. Hence, a more comprehensive and quantitative analysis is required to confirm that a similar approach can be applied to evaluate the effects of a wide variety of process parameters.

Therefore, it is aimed to investigate the effect of the process parameters on the ductile–brittle material response transition and confirm that stress intensity factor analysis can be applied with a wide variety of process parameters. In this study, we observed the characteristics of 8 mol% YSZ in cubic crystal form when subjected to ultra-precision orthogonal cutting. The transition of the material response in plunge cuts was observed and the cutting forces at the ductile–brittle transition point were investigated in terms of a range of process parameters. Then

trends in the cutting force and stress were analyzed and compared with those obtained using a conventional cutting force model. The results of this study enabled us to predict and control the ductile–brittle transition of ceramic during machining with respect to process parameters. With identified crack initiation parameters, crack initiation/propagation could be suppressed, thus enabling us to develop machining strategies with improved process throughput. Furthermore, it is expected that our model can be applied to other ceramic materials with different crystal structures.

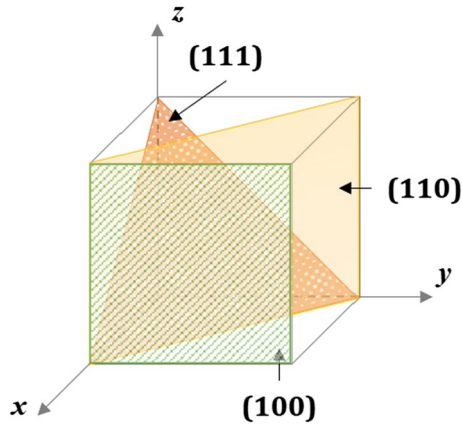


**Fig. 1** Crystal plane system of cubic 8 mol% yttria-stabilized zirconia (YSZ). (reproduced from Yoon et al. [16] with permission from Elsevier.)

## 2 Materials and Methods

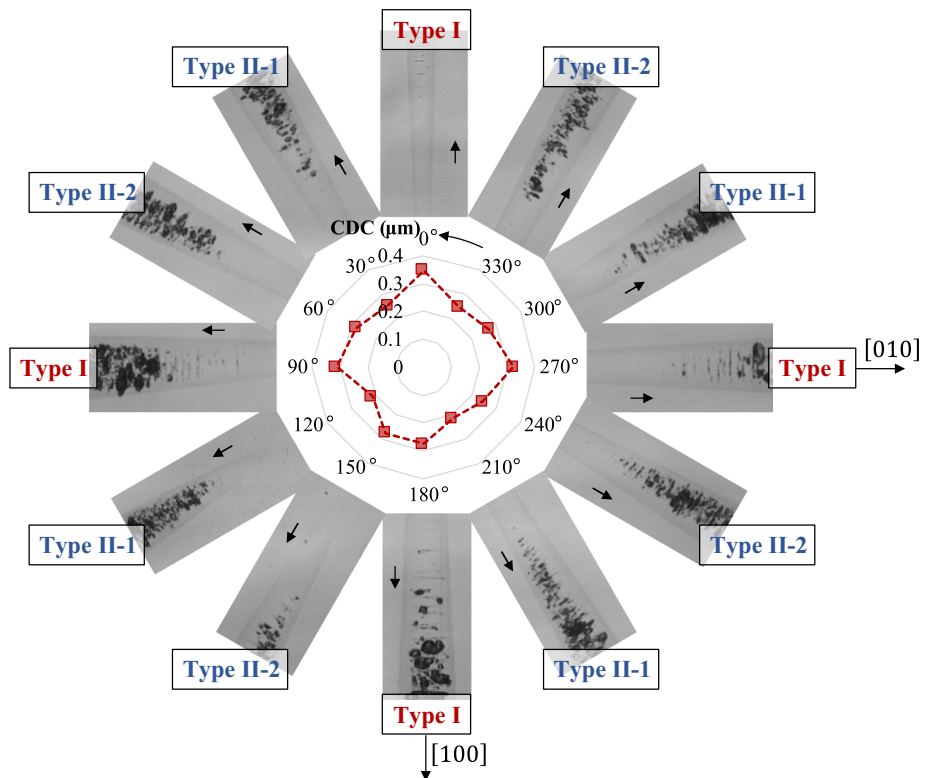
### 2.1 Ductile–Brittle Transition in Ultra-Precision Orthogonal Cutting of Zirconia

Figure 1 shows the crystal plane system of cubic YSZ. Cubic YSZ is known to be a face-centered cubic crystal with {100}, {110}, and {111} planes. In the preliminary study [16], the machining characteristics were observed in different cutting directions along the (001) plane.

To quantitatively analyze the ductile behavior in orthogonal cutting, the critical depth of cut (CDC) was measured. This is the depth at which the first significant cracks occur. Directions with larger CDCs exhibit ductile behavior over longer cutting distances and are thus considered preferred directions for achieving longer ductile regime cutting.

Figure 2 shows the CDCs of different cutting directions, tend to be between 200 and 400 nm. Due to the cubic crystal form of the YSZ, the CDC results exhibited two-fold symmetry, with larger values in the 0°, 90°, 180°, and 270° directions. The characteristics of the CDC and different types of crack morphology (Fig. 3) were discussed in detail in the preliminary study [16]. Here, it has been hypothesized that the stress intensity factor influences the initiation of cracks on different crystal planes simultaneously. The stress intensity factor,  $K_I$ , represents severity for the stress state in crack propagation, and can be calculated as follows:

**Fig. 2** Characteristics of the critical depth of cut (CDC) and classification of crack morphologies with respect to the cutting direction on the (001) plane. (reproduced from Yoon et al. [16] with permission from Elsevier.)



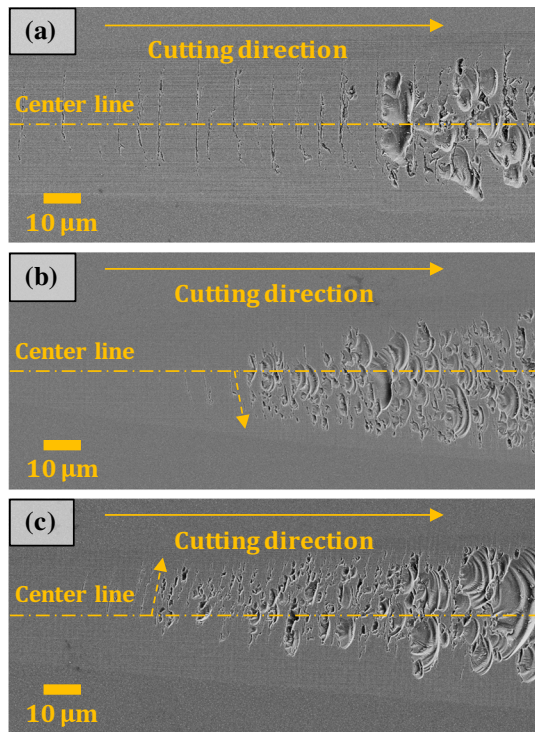


**Fig. 3** Extended view (scanning electron microscope images) of crack morphologies. **a** Type I, **b** Type II-1 and **c** Type II-2 cracks. (reproduced from Yoon et al. [16] with permission from Elsevier.)

$$K_I = G \cdot \sigma_N \cdot \sqrt{\pi a} \quad (1)$$

where  $G$  is a geometric factor that showing the positioning of the initial flaw, and  $a$  is the half of the length of an initial flaw.

In the cutting area, the stress was projected normally to the corresponding crystal plane (or the plane contributing to crack propagation) and then compared with the critical stress intensity factor of that plane. The critical stress intensity factor is a material property and could be found in the literature [17]. It is assumed that cracks would appear if the projected stress reached the critical values. Experimental results found the measured stress to be in good agreement with the values estimated based on the critical stress intensity factor. Thus, we inferred that the CDC can be predicted based on the properties of the material and the geometric relationship between the cutting direction and the crystal plane system.

In addition, the combined effects of various processing conditions were considered in this study. The effects of varying the process parameters was investigated by expressing the experimental results in terms of the cutting force model developed by Günay et al. [18], which was originally suggested by Kienzle and Viktor [19]. Though many models

have been developed, it is still challenging to predict the cutting forces precisely [20], particularly in the case of ultra-precision machining. This is due to the small magnitude of the force itself [21] and the comparable tool edge radius [22, 23]. Here, by measuring the force coefficients directly, an empirical model is expected to provide reliable results and clear insight from the outset. From the literature, the following model was used to predict the main cutting force ( $F_y$ ).

$$F_y = A \cdot k_s \cdot k_v \cdot k_\gamma \cdot k_a \cdot k_t \quad (2)$$

where  $A$  is the cutting area,  $k_s$  is the specific cutting stress,  $k_v$  is the cutting speed factor,  $k_\gamma$  is the rake angle factor,  $k_a$  is the tool wear factor, and  $k_t$  is the tool material factor. The rake angle factor  $k_\gamma$  can be expressed more in detail as follows:

$$k_\gamma = (C - 1.5\gamma)/100 \quad (3)$$

where  $\gamma$  is the effective rake angle in degrees, and  $C$  is the rake angle constant. The literature [18] mentioned that  $C$  values of 103 were used for non-steel materials. It is assumed that the specific cutting stress  $k_s$  would always be the same at the ductile–brittle transition point, regardless of other conditions, because the stress intensity factor is hypothesized to affect crack initiation. To match experimental results with equations, one set of results was measured whilst varying only one parameter, then force values from the model were compared with other sets of experimental results. Following the basic idea put forward by Blake and Scattergood [24], the cutting model includes a plastic deformation zone that forms in front of the face of the tool rake. The shape and size of the plastic deformation zone may vary with the process parameters, but it is still assumed that a crack will occur if the stress on the cutting area exceeds the critical value.

## 2.2 Experimental Details

Figure 4 shows the experimental setup for the orthogonal cutting. A five-axis ultra-precision machine tool, ROBO-NANO  $\alpha$ -0iB (FANUC Corporation, Japan), with a command resolution of one nanometer in the linear axes and one micro-degree in rotary axes was used. Nano-poly-crystalline diamond tools (customized, A.L.M.T. Corp., Japan) were used to cut a double-side-polished mono-crystalline 8 mol% cubic YSZ substrate (MTI Corporation, USA).

Plunge cuts were then performed in the [110] direction on the (001) plane, because, compared to other directions, there was a relatively clear boundary at the ductile–brittle transition point in this direction. Figure 5 shows a schematic image of the plunge cut with a slope of 1/500. During the

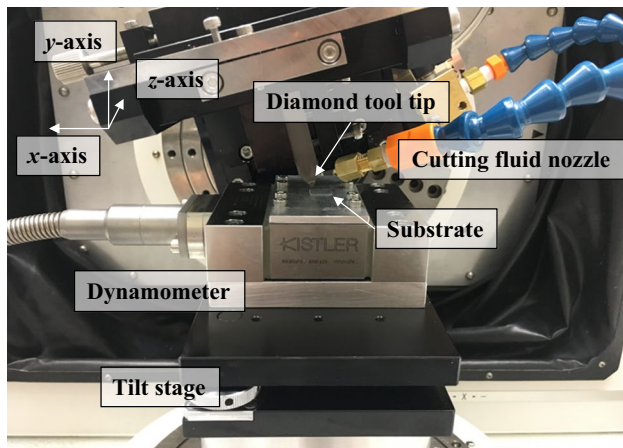


Fig. 4 The experimental configuration

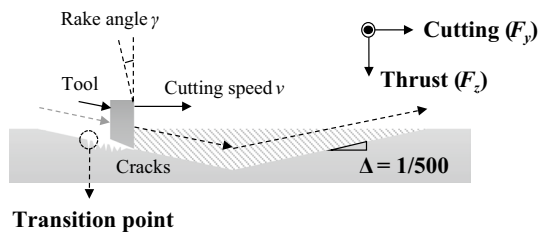


Fig. 5 Schematic diagram of the tool path

cutting, a dynamometer (Type 9119AA1, Kistler Inst. Corp., Switzerland) and multi-channel amplifier (Type 5080A, KISTLER Instrument Corp.) measured the signals for the cutting force. A sampling frequency of 20000 Hz was used, and a low pass filter was applied to the signal with a cut-off frequency of 5000 Hz.

A variety of process parameters were used in this set of experiments, as shown in Table 1. Two diamond tools with the same geometry but different nose radius were used (Fig. 6). Zero- and negative rake angles were used to protect the tip of the tool from damage at the moment of contact. Cutting speeds were also selected in a range of 5–20 mm min<sup>-1</sup>.

Figure 7 shows examples of machined slots from the top view. As the dominant material behavior changed with the depth of cut, the surface also changed from a clean

ductile region to a brittle region with numerous conchoidal cracks. More examples are shown in Fig. 7a, b; thin-dashed lines are plotted together to show the machined area clearly. The sample shown in Fig. 7a, obtained with a cutting speed of 10 mm min<sup>-1</sup>, had a relatively small ductile area compared to that of Fig. 7b, where a higher cutting speed of 20 mm min<sup>-1</sup> was used. Then, similar to the previous study [16], the CDC was measured for different cutting directions to quantitatively compare the machining characteristics.

The cutting forces also differed clearly with respect to the dominant material behavior. Figure 8 shows the cutting force signal measured when making the cut shown in Fig. 7a. The cutting forces gradually increased as the depth of the cut increased within the ductile regime. Cracks started to open after the dominant material response transitioned from the ductile regime to the brittle regime, and the forces also vibrated significantly more. In this case, the  $F_y$  vibrated more than the thrust force ( $F_z$ ) because the cracks opened in the same direction as the cutting direction [110]. The vibrations of the forces also matched the surface morphologies observed in the optical images well. The ductile–brittle transition points were identified by combining optical images with the cutting force signals.

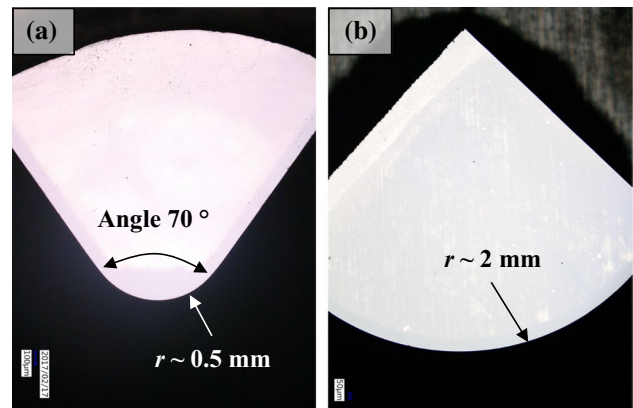
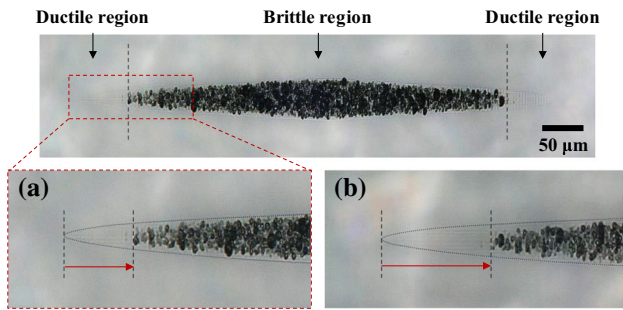


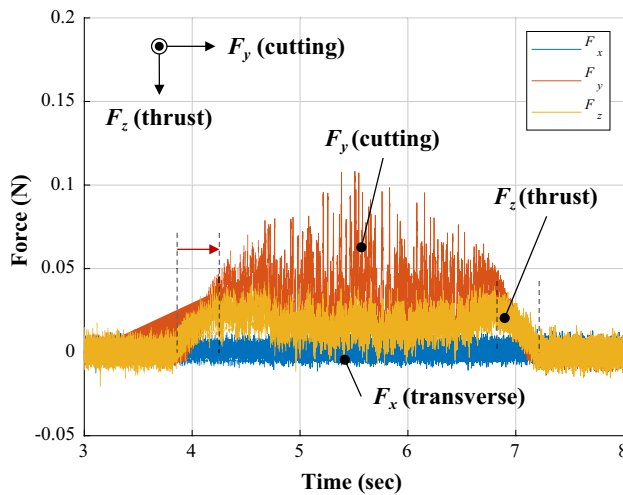
Fig. 6 Two different diamond tools a with a nose radius of 0.5 mm and b with a nose radius of 2 mm

Table 1 Process parameters used in the experiments

Items	Parameters values
Cutting tool	Nano-polycrystalline diamond tools with nose radius of (1) 0.5 mm (Tool #1) and (2) 2 mm (Tool #2).
Rake angle (°)	0, -5, -10
Cutting speed (mm min <sup>-1</sup> )	5, 10, 15, 20



**Fig. 7** An example of a machined slot in cutting direction [110] with a cutting speed of **a** 10 mm min<sup>-1</sup> and **b** 20 mm min<sup>-1</sup>. The rake angle was 0°



**Fig. 8** An example of the cutting force signal

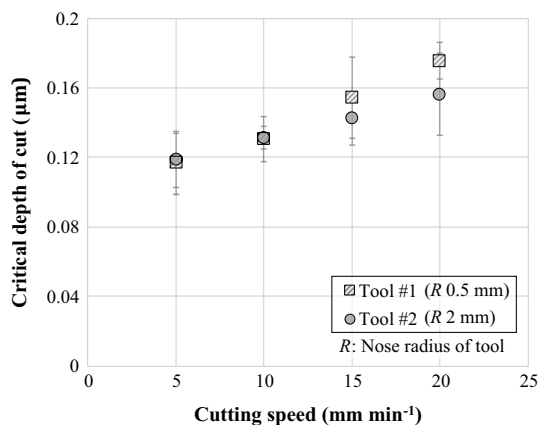


**Fig. 9** The CDC with respect to the cutting speed for two different tools

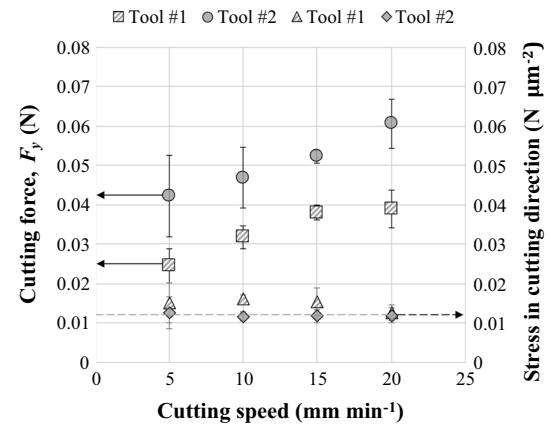


**Fig. 10** Cutting forces ( $F_y$ ) and stress in the cutting direction at the ductile–brittle transition point for the two different tools

## 3 Results and Discussion

### 3.1 Effects of Cutting Tools

Figure 9 shows the CDC results with respect to the cutting speed for the two different tools shown in Fig. 6. Seeing the results, both tools gave similar CDCs at each cutting speed, ranging from 0.12 to 0.18  $\mu\text{m}$ . However, this does not imply that both tools have similar manufacturability. Tool #2 had a larger cutting area due to its larger tool nose radius (2 mm). This means that the cutting area of Tool #2 was about twice that of Tool #1 (nose radius of 0.5 mm) when the depth of cut was 0.120  $\mu\text{m}$ .

The cutting force increased with the cutting area of the tool at the ductile–brittle transition point. Figure 10 shows the main cutting forces  $F_y$  and the stress in the cutting direction at the ductile–brittle transition. Here, instead of the stress intensity factor, simply the stress in the cutting direction (y-direction) was calculated and compared, as the cutting direction is fixed in [110]. All other factors such as  $G$  and  $a$  in Eq. 1 are the same regardless of processing conditions, hence the stress intensity factor is influenced only by the stress.

As explained in Sect. 2, the main cutting force is expected to be proportional to the cutting area  $A$  (Eq. 2). The cutting force gradually increased with the cutting area, and the difference between the cutting forces of Tools #1 and #2 was exactly proportional to the ratio of the cutting areas, rather than the magnitudes of the forces themselves.

Thus, the stress showed the similar value, of approximately 0.011  $\text{N } \mu\text{m}^2$ , regardless of the difference between the tool nose radius. Thus, it can be inferred that expanding the cutting area in the transverse direction (rather than in the cutting or thrust direction) does not affect the stress status or plastic deformation zone, and the material removal rate

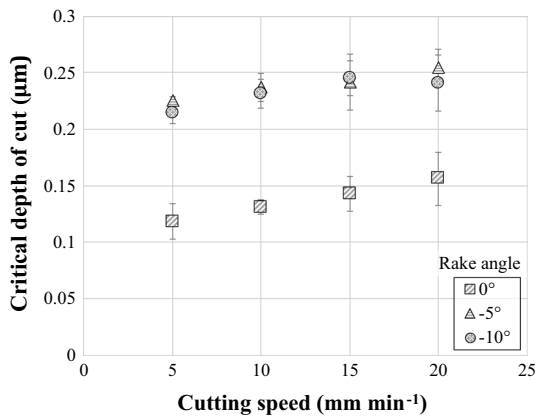


Fig. 11 The CDC in terms of the cutting speed with respect to different rake angles. Tool #2 was used

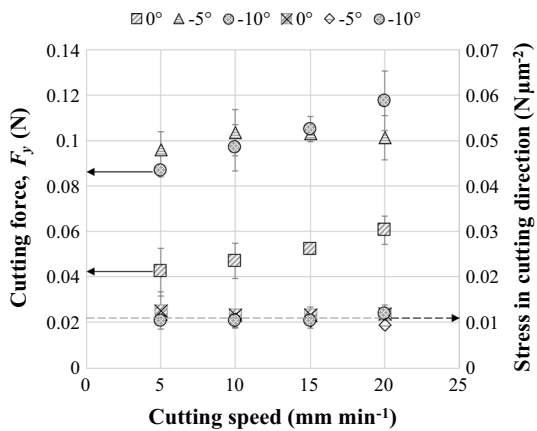


Fig. 12 The  $F_y$  and stress in the cutting direction at the ductile–brittle transition point with respect to different rake angles

can be increased by simply adopting tools with wider cutting areas. Meanwhile, the cutting speed had a large influence on the CDC. The effect of the cutting speed is discussed in more detail in the next section.

### 3.2 Effects of Varying the Process Parameters

Figure 11 shows the CDC results with respect to the cutting speed for different tool rake angles. The CDC increased dramatically as the rake angle decreased from 0° to −5°, but the difference in CDC as the rake angle decreased from −5° and −10° was much less significant. Similar to the former set of experiments, the overall CDC increased as the cutting speed increased, but the CDC increased from 0.04 to 0.05 μm when the cutting speed increased from 5 to 20 mm min<sup>-1</sup> and those differences remained similar regardless of the rake angle.

To analyze the material response in more detail, cutting forces were investigated simultaneously. Figure 12 shows the main cutting forces and the stress in cutting direction at

the moment of ductile–brittle transition. Seeing the figure, stress in cutting direction remained similar regardless of the rake angle or cutting speed, and its value, 0.011 N μm<sup>2</sup>, was even similar to the stress shown in Fig. 10. This result supports our hypothesis that crack initiation is predominantly influenced by the stress intensity factor. As the cutting direction [110] in this set of experiments was the same as the crack-initiation direction (tensile) on the plane (110), these results also support the hypothesis that, at the ductile–brittle transition point, the specific cutting stresses ( $k_s$ ) in the model (Eq. 2) are the same as the value derived from the critical stress intensity factor. The stress in the cutting direction did not vary with any of the process parameters that adjusted here, *i.e.*, the tool nose radius, rake angle, and cutting speed.

On the other hand, the cutting speed had a negligible direct effect on the cutting force within the range of parameters used in these experiments. Considering the increase in the CDC, the differences in forces were only due to the change in the cutting area. As it is assumed that the crack-initiation direction and  $k_s$  remained constant, the force remained proportional to the cutting area for as long as the crack-initiation mode was maintained.

The increase in the cutting speed was thought to be just the factor influencing the increase in the CDC, rather than directly influencing the force itself at the ductile–brittle transition point. The decrease in the effective rake angle and friction during the cutting at higher cutting speeds are thought to increase the extent of the plastic deformation zone in front of the tool rake face, thus to increase the CDC. Nevertheless, the expansion of the plastic deformation zone will be limited, so increasing the cutting speed will eventually cause the CDC to converge to a specific value. Also, the material will not have an infinite CDC. Chen et al. [25] measured the CDCs of single crystal calcium fluoride (CaF<sub>2</sub>) and found that they differed by less than 100 nm, even with cutting speeds ranging from 2000 to 4000 mm min<sup>-1</sup>. Nonetheless, within the range of these experiments, the CDC increased significantly when the cutting speed increased, and the ductile–brittle transition point could be predicted in terms of the cutting stress.

Then the effect of varying the rake angle was analyzed, using Eq. 2 to formulate an empirical model based on the experimental results. The effect of the rake angle was simply considered as a ratio, using numbers calculated with Eq. 3. Figure 13 shows a comparison between the measured main cutting forces and the values estimated from the model. The experimental values were much larger than the estimated values. The results for rake angles −5° and −10° were approximately double those for 0° rake angle, while the model suggested that the main cutting force would increase by about 7–14%.

The increase in the cutting force was much higher than other results reported in the literature. In the experiments

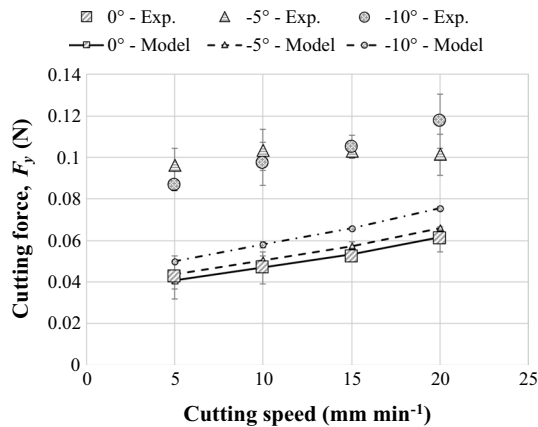


**Fig. 13** Values of  $F_y$  obtained experimentally and predicted by the model

carried out by Günay et al. [18]., the cutting force increased by 2% as the rake angle decreased from  $0^\circ$  to  $-5^\circ$ . Although they used AISI 1040 steel as their material, it is hard to explain the approximate doubling of the force in terms of conventional orthogonal cutting models.

On the contrary, similar trends have been reported with the cutting of ceramic materials [25]. Calcium fluoride had a CDC of over 600 nm with negative rake angles, even though it was less than 200 nm with a rake angle of  $0^\circ$ . Comparing to usual metal cutting cases leads us to expect a sudden change in the effective rake angle within this range. The large compressive stress caused by the negative rake angle enlarges the plastic deformation zone in front of the tool rake face [26] and is thought to suppress crack propagation inside the surface. The effect of the rake angle on ductile cutting behavior may vary depending on the material [27], but it is effective enough at enlarging the CDC, at least in the case of zirconia.

However, if the rake angle is too negative then subsurface damage may occur when the material recovers after the tool has passed over it [8]. Hence, this situation should be avoided. The distribution of the  $F_y$  and  $F_z$  also changed significantly when the rake angle became negative. This provides further evidence of the change in the plastic deformation zone. The ratio of the  $F_z$  to the cutting force increased suddenly as the rake angle decreased from  $0^\circ$  to  $-5^\circ$ , as shown in Fig. 14. In the case of the cutting speed of  $5 \text{ mm min}^{-1}$ , the angle formed by the  $F_y$  and  $F_z$  increased from about  $23^\circ$  to  $38^\circ$ . It is therefore required to consider different force models for different tool rake angles, particularly near  $0^\circ$ . Nevertheless, the value of the stress in the cutting direction remained constant, regardless of the process parameters.

Combining all of these results enables us to predict the ductile–brittle transition point with respect to the cutting stress. First, our experimental results showed that the

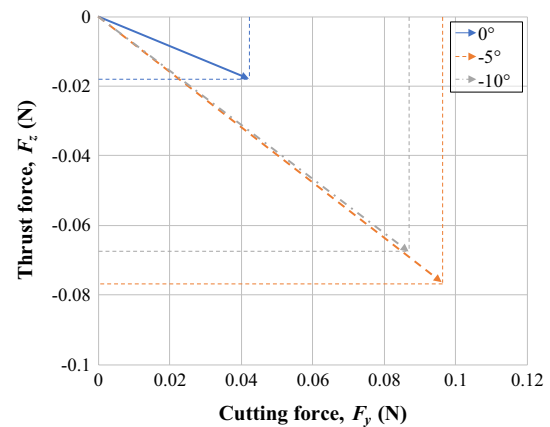


**Fig. 14** Distribution of the  $F_y$  and thrust force ( $F_z$ ) with respect to the rake angle

specific cutting stress at the ductile–brittle transition point remained constant, regardless of the tool nose radius, rake angle, and cutting speed. Hence, the ductile–brittle transition point can be predicted by monitoring the stress in the direction normal to the corresponding crystal plane. Second, effects of varying the process parameters on the CDC were investigated. Higher cutting speeds brought the extent of the plastic deformation zone forwards, thus causing higher CDC values. The cutting force at the ductile–brittle transition point was proportional to the cutting area at that moment. Negative rake angles created compressive pressure in front of the tool, and also improved the CDC in comparison to the  $0^\circ$  rake angle. It was not easy to predict the cutting forces with negative rake angles directly, because the downward compressive force changed the deformation zone dramatically. However, our experimental results enabled to roughly estimate that the CDC for negative rake angles above  $-10^\circ$  would be similar in value to the CDC for rake angles of  $-5^\circ \sim -10^\circ$ , because the difference between the CDCs at rake angles of  $-5^\circ$  and  $-10^\circ$  was almost negligible. More research is required to formulate a model to predict the response of the material during the cutting, particularly regarding the changes in the deformation zone with respect to other process parameters. Nevertheless, it is still believed that the specific cutting stress will remain constant at the ductile–brittle transition point.

## 4 Conclusions

In this study, the processing of cubic YSZ was investigated. The results of our preliminary study suggested that the stress intensity factor influences crack initiation on different crystal planes simultaneously. Here, experiments were performed to confirm that the stress intensity factor analysis can be applied with a wide variety of process parameters, and to



investigate the effect of varying the process parameters on the ductile–brittle material response transition.

Experimental results strongly supported our hypothesis that the stress intensity factor influences the crack initiation on crystal planes. Regardless of the change in tool nose radius, rake angle, and cutting speed, the value of the cutting stress at the ductile–brittle transition point remained constant as the crack-initiation plane and opening mode (tensile) were maintained. Higher cutting speeds and negative rake angles are thought to enlarge the extent of the plastic deformation zone in front of the tool rake face, thus increasing the ductile cutting length. The cutting force at the ductile–brittle transition point is proportional to the area at that moment. It will be necessary to assess the changes in the shear zone and material deformation during cutting in detail so that the machining characteristics can be explained more clearly.

Based on experimental results and investigation in this study, more research will be performed in both analytical and numerical ways. Nonetheless, this study confirmed that stress intensity factor analysis is an effective method for predicting the ductile–brittle transition in cutting and can be applied to provide insights into the effects of varying different process parameters. It is expected this research can contribute to the development of new machining strategies with improved throughput, either by suppressing the stress in the crack-opening direction, or by increasing the critical stress intensity factors of the materials themselves, and thus, contribute to an increase in the utilization of ceramic materials.

**Acknowledgements** Authors gratefully acknowledge kind support from the FANUC Corporation, Japan, for the loan of the 5-axis ultra-precision machine tool, ROBONANO  $\alpha$ -0iB, and A.L.M.T. Corp., Japan, for providing PCD tools to MIN LAB at UW-Madison. This work was also supported by the National Research Foundation of Korea (NRF) grant funded by the Ministry of Education, Science and Technology (Nos. NRF-2018R1C1B5085752 and NRF-2016R1A6A3A03012011), and 2018 Korea Aerospace University Faculty Research Grant.

## References

- Liu, Z. Y., Huang, C., Zhao, Y., & Guo, Y. B. (2017). Kinematic modeling and deformation mechanics in shot peening of functional ceramics. *International Journal of Advanced Manufacturing Technology*, 93(5–8), 1669–1683. <https://doi.org/10.1007/s00170-017-0661-y>.
- Ferraris, E., Vleugels, J., Guo, Y., Bourell, D., Kruth, J. P., & Lauwers, B. (2016). Shaping of engineering ceramics by electro, chemical and physical processes. *CIRP Annals*, 65(2), 761–784. <https://doi.org/10.1016/j.cirp.2016.06.001>.
- Anselmi-Tamburini, U., Woolman, J. N., & Munir, Z. A. (2007). Transparent nanometric cubic and tetragonal zirconia obtained by high-pressure pulsed electric current sintering. *Advanced Functional Materials*, 17(16), 3267–3273. <https://doi.org/10.1002/adfm.200600959>.
- Hannink, R. H. J., Kelly, P. M., & Muddle, B. C. (2000). Transformation toughening in zirconia-containing ceramics. *Journal of the American Ceramic Society*, 83(3), 461–487. <https://doi.org/10.1111/j.1151-2916.2000.tb01221.x>.
- Schelling, P. K., Phillpot, S. R., & Wolf, D. (2001). Mechanism of the cubic-to-tetragonal phase transition in zirconia and yttria-stabilized zirconia by molecular-dynamics simulation. *Journal of the American Ceramic Society*, 84(7), 1609–1619. <https://doi.org/10.1111/j.1151-2916.2001.tb00885.x>.
- Pfefferkorn, F. E., Shin, Y. C., Tian, Y., & Incropera, F. P. (2004). Laser-assisted machining of magnesia-partially-stabilized zirconia. *Journal of Manufacturing Science and Engineering*, 126(1), 42–51. <https://doi.org/10.1115/1.1644542>.
- Pashmforoush, F., & Esmailzare, A. (2017). Experimentally validated finite element analysis for evaluating subsurface damage depth in glass grinding using Johnson-Holmquist model. *International Journal of Precision Engineering and Manufacturing* 18(12), 1841–1847. <https://doi.org/10.1007/s12541-017-0213-2>.
- Neo, W. K., Kumar, A. S., & Rahman, M. (2012). A review on the current research trends in ductile regime machining. *International Journal of Advanced Manufacturing Technology*, 63(5–8), 465–480. <https://doi.org/10.1007/s00170-012-3949-y>.
- Maas, P., Mizumoto, Y., Kakinuma, Y., & Min, S. (2017). Machinability study of single-crystal sapphire in a ball-end milling process. *International Journal of Precision Engineering and Manufacturing* 18(1), 109–114. <https://doi.org/10.1007/s12541-017-0013-8>.
- Zhang, G., Zeng, Y., Zhang, W., Zhou, H., Wen, Z., & Yao, Y. (2016). Monitoring for damage in two-dimensional pre-stress scratching of SiC ceramics. *International Journal of Precision Engineering and Manufacturing* 17(11), 1425–1432. <https://doi.org/10.1007/s12541-016-0168-8>.
- Chen, J. B., Fang, Q. H., Wang, C. C., Du, J. K., & Liu, F. (2016). Theoretical study on brittle–ductile transition behavior in elliptical ultrasonic assisted grinding of hard brittle materials. *Precis Engineering* 46, 104–117. <https://doi.org/10.1016/j.precisiong.2016.04.005>.
- Venkatachalam, S., Li, X., & Liang, S. Y. (2009). Predictive modeling of transition undeformed chip thickness in ductile-regime micro-machining of single crystal brittle materials. *Journal of Materials Processing Technology*, 209(7), 3306–3319. <https://doi.org/10.1016/j.jmatprotec.2008.07.036>.
- Arif, M., Xinquan, Z., Rahman, M., & Kumar, S. (2013). A predictive model of the critical undeformed chip thickness for ductile–brittle transition in nano-machining of brittle materials. *International Journal of Machine Tools and Manufacture* 64, 114–122. <https://doi.org/10.1016/j.ijmachtools.2012.08.005>.
- Mizumoto, Y., Maas, P., Kakinuma, Y., & Min, S. (2017). Investigation of the cutting mechanisms and the anisotropic ductility of monocrystalline sapphire. *CIRP Annals*, 66(1), 89–92. <https://doi.org/10.1016/j.cirp.2017.04.018>.
- Yoon, H.-S., Kwon, S. B., Nagaraj, A., Lee, S., & Min, S. (2018). Study of stress intensity factor on the anisotropic machining behavior of single crystal sapphire. *CIRP Annals*, 67(1), 125–128. <https://doi.org/10.1016/j.cirp.2018.04.114>.
- Yoon, H.-S., Lee, S., & Min, S. (2018). Investigation of ductile–brittle transition in machining of yttrium-stabilized zirconia (YSZ). In *Procedia Manufacturing, 46th SME North American manufacturing research conference, NAMRC 46, Texas, USA* (Vol. 26, pp. 446–453). <https://doi.org/10.1016/j.promfg.2018.07.052>.
- Pajares, A., Guiberteau, F., Dominguez-Rodriguez, A., & Heuer, A. H. (1988). Microhardness and fracture toughness anisotropy in cubic zirconium oxide single crystals. *Journal of the American Ceramic Society*, 71(7), 332–333. <https://doi.org/10.1111/j.1151-2916.1988.tb05933.x>.

18. Günay, M., Aslan, E., Korkut, I., & Seker, U. (2004). Investigation of the effect of rake angle on main cutting force. *International Journal of Machine Tools and Manufacture*, 44(9), 953–959. <https://doi.org/10.1016/j.ijmachtools.2004.01.015>.
19. Kienzle, O., & Victor, H. (1957). Spezifische Schnittkräfte bei der Metallbearbeitung. *Werkstattstechnik und Maschinenbau*, 47(5), 224–255.
20. Grossi, N. (2017). Accurate and fast measurement of specific cutting force coefficients changing with spindle speed. *International Journal of Precision Engineering and Manufacturing* 18(8), 1173–1180. <https://doi.org/10.1007/s12541-017-0137-x>.
21. Yoon, H.-S., Wu, R., Lee, T.-M., & Ahn, S.-H. (2011). Geometric optimization of micro drills using Taguchi methods and response surface methodology. *International Journal of Precision Engineering and Manufacturing* 12(5), 871–875. <https://doi.org/10.1007/s12541-011-0116-6>.
22. Kim, C.-J., Mayor, R., & Ni, J. (2012). Molecular dynamics simulations of plastic material deformation in machining with a round cutting edge. *International Journal of Precision Engineering and Manufacturing* 13(8), 1303–1309. <https://doi.org/10.1007/s12541-012-0173-5>.
23. Luo, S., Bayesteh, A., Ko, J., Dong, Z., & Jun, M. B. (2017). Numerical simulation of chip ploughing volume in micro ball-end mill machining. *International Journal of Precision Engineering and Manufacturing*, 18(7), 915–922. <https://doi.org/10.1007/s12541-017-0108-2>.
24. Blake, P. N., & Scattergood, R. O. (1990). Ductile-regime machining of germanium and silicon. *Journal of the American Ceramic Society*, 73(4), 949–957. <https://doi.org/10.1111/j.1151-2916.1990.tb05142.x>.
25. Chen, X., Xu, J., Fang, H., & Tian, R. (2017). Influence of cutting parameters on the ductile-brittle transition of single-crystal calcium fluoride during ultra-precision cutting. *International Journal of Advanced Manufacturing Technology*, 89(1–4), 219–225. <https://doi.org/10.1007/s00170-016-9063-9>.
26. Yan, J., Syoji, K., Kuriyagawa, T., & Suzuki, H. (2002). Ductile regime turning at large tool feed. *Journal of Materials Processing Technology*, 121(2–3), 363–372. [https://doi.org/10.1016/S0924-0136\(01\)01218-3](https://doi.org/10.1016/S0924-0136(01)01218-3).
27. Wang, J.-J. J., & Liao, Y.-Y. (2007). Critical depth of cut and specific cutting energy of a microscribing process for hard and brittle materials. *Journal of Engineering Materials and Technology*, 130(1), 011002–011002–6. <https://doi.org/10.1115/1.2806253>.

**Publisher's Note** Springer Nature remains neutral with regard to jurisdictional claims in published maps and institutional affiliations.



**Hae-Sung Yoon** is currently an Assistant Professor in the School of Aerospace and Mechanical Engineering at Korea Aerospace University (KAU), Korea. He received his B.S. in 2010, and Ph.D. in 2015 (M.S. integrated) all in Mechanical and Aerospace Engineering from Seoul National University, Korea. Since then, he has held professional positions as a Postdoctoral Fellow in BK21+ Program at Seoul National University from 2015 to 2016, and as a Research

Associate in the Department of Mechanical Engineering at University of Wisconsin-Madison, USA, from 2016 to 2018. Yoon's research interests are in Hybrid/Smart Manufacturing, Sustainable Manufacturing, Ultra-precision Machining, Micro/Nano Fabrication, 3D/4D Printing, Manufacturing for Design, and Smart Materials.



**Suk Bum Kwon** Ph.D. candidate in the Department of Mechanical Engineering, University of Wisconsin-Madison, Wisconsin, United States. His research interest includes ultra-precision machining of ceramics.



**Aditya Nagaraj** He received the M.S. degree in Manufacturing Systems Engineering from the University of Wisconsin-Madison, USA. His research interests include ultra-precision machining of single crystalline ceramics.



**Sangkee Min** is currently an assistant professor at Department of Mechanical Engineering, University of Wisconsin-Madison. He received Ph.D. in 2001 at U.C. Berkeley. He has been working on machining processes, burr formation, and smart manufacturing, and MFD (Manufacturing for Design).